Available online at www.sciencedirect.com
ScienceDirect
Journal of Power Sources 173 (2007) 149–155
JOURNAL OF POWER SOURCES
www.elsevier.com/locate/jpowsour

Operating characteristics of direct methanol fuel cell using a platinum–ruthenium catalyst supported on porous carbon prepared from mesophase pitch

Kidon Nam [a,b], Doohwan Jung [a,*], Sang-Kyung Kim [a], Donghyun Peck [a], Seungkon Ryu [b]

[a] *Advanced Fuel Cell Research Center, Korea Institute of Energy Research, 71-2 Jang-dong, Yuseong-gu, Daejeon 305-343, Republic of Korea*
[b] *Department of Chemical Engineering, Chungnam National University, 220 Gung-dong, Yuseong-gu, Daejeon 305-764, Republic of Korea*

Received 15 February 2007; accepted 16 April 2007
Available online 27 April 2007

Abstract

The characteristics of a platinum–ruthenium catalyst supported on porous carbon (PC) are analysed by X-ray diffraction, scanning electron microscopy, cyclic voltammetry and chemisorption techniques. Single-cell tests are carried out in order to compare the performance of these catalysts as an anode in a direct methanol fuel cell with respect to that of a commercial-grade catalyst. The methanol oxidation rate on a Pt–Ru catalyst supported on PC with a pore size of 20 nm is about 35% higher than that on a commercial E-TEK catalyst. The catalyst (Pt–Ru/K20) in the single-cell test gives a power density of 90 and 126 mW cm^{-2} under air and oxygen at 60 °C, respectively. These values are 15–16% higher than those obtained with a commercial E-TEK catalyst.

Keywords: Direct methanol fuel cell; Porous carbon; Cyclic voltammetry; Single-cell test; Platinum–ruthenium catalyst, Power density

1. Introduction

Porous carbons (PCs) with good electronic conductivity have been widely used as a catalyst supports and electrodes in fuel cells, purification processes, chromatographic separations and adsorbents [1,2]. Many techniques such as activation, templating methods and sol–gel techniques have been proposed to make controllable PCs [2]. The preparation of PCs with controllable meso- and macropores as catalyst supports is extremely important for fuel cells. Johnson et al. [3] reported the synthesis of mesoporous polymers with a pore size of ∼50 nm using close-packed silica nanoparticles as templates. Using such templates, porous materials with spherical pore structures have been synthesized. Other workers [4–6] studied highly ordered, uniform, porous carbon as a catalyst support with colloidal silica templates by the carbonization of phenol and formaldehydes as a carbon precursor in the presence of sulfuric acid. They found much improved catalytic activity for methanol oxidation in a fuel cell. This is most likely due to their three-dimensionally interconnected, uniform, pore structures and large surface area. Kim and co-workers [7,8] studied mesocellular carbon foams and ordered mesoporous carbon materials with larger surface areas that were synthesized via direct carbonization of synthesized silica/cross-linked, triblock, copolymer nanocomposites through acid-catalyzed sol–gel polymerization.

In the present study, porous carbons with a controlled pore size are prepared as a catalyst support material for anode electrodes from naphthalene-based mesophase pitch with silica spheres. To serve an anode electrode catalyst for a direct methanol fuel cell (DMFC), 60 wt.% of Pt–Ru metals is loaded on the porous carbon (PC).

The characteristics and surface morphology of PCs with Pt–Ru catalysts are determined through the use of a scanning electron microscopy (SEM) and specific surface-area analysis (BET) [1,2,9]. The characteristics and activities of the Pt–Ru catalyst supported on PCs are analyzed by X-ray diffraction (XRD) [10–14], cyclic voltammetry [15,16] and chemisorption techniques. Single-cell tests [17,18] are carried out to compare the performance of the anode electrode in the DMFC using the

* Corresponding author. Tel.: +82 42 860 3577; fax: +82 42 860 3309.
E-mail address: doohwan@kier.re.kr (D. Jung).

0378-7753/$ – see front matter © 2007 Published by Elsevier B.V.
doi:10.1016/j.jpowsour.2007.04.055

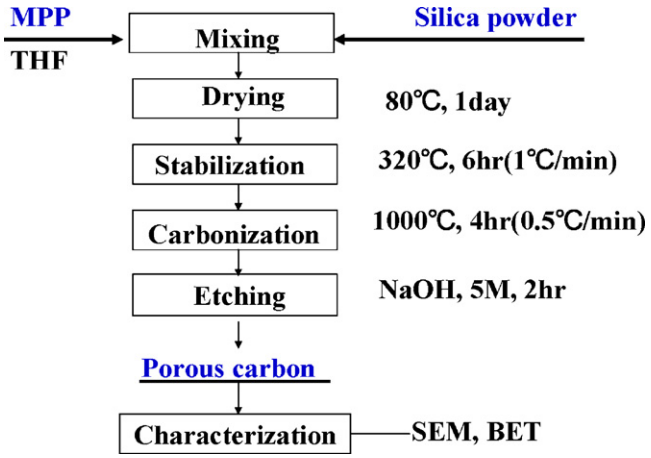

Fig. 1. Manufacturing process of PC using mesophase pitch (MPP) with silica powder.

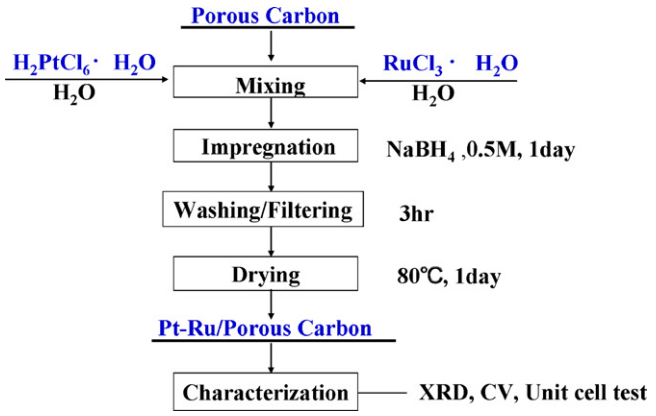

Fig. 2. Preparation of Pt–Ru catalyst supported on PC.

catalysts supported on PCs with that of a commercial grade catalyst.

2. Experimental

2.1. Manufacture of porous carbons

The manufacturing process of the porous carbon based on mesophase pitch (AR, Mitsubishi Chemical) [18]. Mesophase pitch dissolved in tetrahydrofuran (THF) was mixed with a prepared silica powder (particle size from 10 to 100 nm) at room temperature for 24 h and then dried at 80 °C in a vacuum chamber for 24 h.

The silica-mixed mesophase pitches were stabilized at 320 °C for 6 h in air and carbonized at 1000 °C for 4 h under a nitrogen atmosphere. The silica in the carbonized material was etched using a NaOH solution and then the material was washed several times with pure water.

The PCs were designated as K100, K50, K20 or K10 depending on the particle size of the dried colloidal silica.

The pore size and nitrogen adsorption capability of the PCs were characterized via SEM (HITACHI S-4700) and BET (ASAP 2010) techniques (Fig. 1).

2.2. Preparation of Pt–Ru/PCs catalysts

The preparation process of the Pt–Ru catalyst supported on PC for the DMFC anode is shown in Fig. 2 [18,19]. $H_2PtCl_6{\cdot}6H_2O$ (Aldrich) and $RuCl_3{\cdot}3H_2O$ (Aldrich) were used as the precursors of the catalysts. The PCs were mixed with $H_2PtCl_6{\cdot}6H_2O$ (Aldrich) and $RuCl_3{\cdot}3H_2O$ (Aldrich) in deionized water. The mixed solution was stirred for 12 h and the PCs were impregnated with Pt–Ru metals using a 0.5 M $NaBH_4$ solutions as a reduction agent for 1 h. After the impregnation, the PC solutions with Pt–Ru metals were filtered and dried at 80 °C for 24 h.

The particle size and characteristics of the Pt–Ru catalyst supported on the PCs were measured using SEM, XRD (Rigaku C., RINT2000) and chemisorption techniques.

2.3. Performance tests of Pt–Ru/PCs catalysts [11,18,20]

The methanol oxidation rate and cell performance were measured by cyclic voltammetry (CV) and single-cell test methods.

To measure the methanol electro-oxidation activity of Pt–Ru/PCs, CV tests were conducted between −0.2 and 1.0 V (versus Ag/AgCl) at a sweep rate of 5 mV s^{-1}. The CV tests were conducted at 30 °C with a 0.5 M H_2SO_4 + 1 M CH_3OH electrolyte. The amount of metal catalyst loaded on the carbon paper was controlled at 2 mg cm^{-2}.

For the single-cell performance test, formulations of 40 wt.% Pt–20 wt.% Ru binary catalyst supported on PC created by the Korean Institute of Energy Research and Pt black (Johnson Matthey HiSPEC 1000) were used as the anode and cathode catalysts, respectively. These catalysts were mixed homogeneously with a Nafion solution (5 wt.%) and water. In order to prepare the catalyst layer, appropriate amounts of anode and cathode ink were uniformly applied to carbon paper of 1.7 cm × 1.7 cm size to give a catalyst loading of approximately 3 mg cm^{-2}, and then dried at 80 °C for 1 h.

The Nafion (115) membrane was cleaned and converted into the acidic form by boiling it in 3% H_2O_2, deionized water, 5% H_2SO_4, and then deionized water again for over 1 h for each step. The membrane-electrode assembly (MEA) was fabricated by hot pressing the surfaces of the anode and cathode electrodes at a temperature of 135 °C and a pressure of 100 kg cm^{-2} for 10 min. The MEA was inserted into the fuel cell hardware, which consisted of a graphite block with a machined serial flow-channel, copper current-collectors, and stainless-steel compression plates. A 2.0 M methanol solution was pumped into the anode channel of the cell, and air was supplied to the cathode channel. Cell performances were evaluated at room temperature to 60 °C.

2.4. Durability tests

A durability test of a single-cell was carried out at a constant current density of 80 mA cm^{-2} with 1.0 M methanol solution as the anode fuel and air as the cathode reactant, at atmospheric pressure. The cell was operated more than 1700 h with a flow rate of 1.0 cm^3 min^{-1} on the anode side and 300 cm^3 min^{-1} on

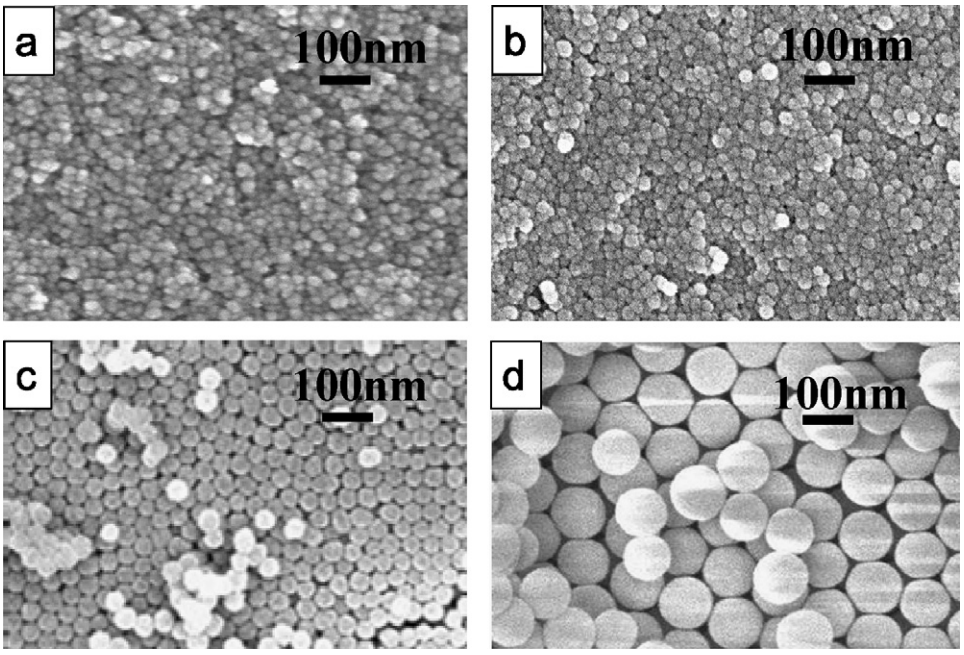

Fig. 3. Electron micrographs of silica spheres: (a) 10–20 nm (CH_3OH/TEOS: 46); (b) 20–30 nm (CH_3OH/TEOS: 42); (c) 40–50 nm (CH_3OH/TEOS: 38); (d) 80–100 nm, (CH_3OH/TEOS: 32).

the cathode side [21]. In addition, commercial-grade Johnson Matthey (HiSPEC 6000) catalyst supported on carbon black (Vulcan XC 72R) was tested under the same conditions for comparison of the characteristics of the durability test results.

3. Result and discussion

3.1. Morphologies and characteristics of porous carbons

Scanning electron micrographs of the silica spheres are shown in Fig. 3. When the silica spheres were created using sol–gel methods, the sizes of the silica spheres were very dependent on the molar ratio of CH_3OH/TEOS [18]. As shown in Fig. 3, when the molar ratios of CH_3OH/TEOS are approximately 46 and 42, well-dispersed silica spheres measuring approximately 10–20 and 20–30 nm in particle size, respectively, are obtained. In addition, as the molar ratios of CH_3OH/TEOS are decreased to 38 and 32, the size of silica spheres becomes 40–50 and 80–100 nm, respectively.

Scanning electron micrographs of carbonized pitch with silica are given in Fig. 4. The size-controlled silica spheres are well dispersed with the carbonized pitch.

Scanning electron micrographs of PCs after etching of the silica spheres by NaOH solution from the carbonized pitch are presented in Fig. 5. Some open pores develop after the heat treatment and the etching process. This is due to the escape of organic materials with low molecular weight from the mesophase pitch during the stabilization and carbonization processes. Additionally, some open pores are formed through the aggregation of silica at nearly 800 °C during the carbonization process [22].

Nitrogen adsorption isotherms of the carbonized PCs are shown in Fig. 6. The results are summarized in Table 1. The specific surface areas of K10, K20, K50 and K100 are 273.2, 212.4, 132.9 and 88.2 $m^2\ g^{-1}$, respectively. The corresponding average pore diameters are 16.9, 17.7, 37.0 and 80.8 nm. Although the specific surface areas of these PCs are relatively low, the meso- to macro-pore ratio becomes 85–90% on the addition of the silica spheres. The pore sizes of the PCs are slightly smaller than the particle sizes of the original silica spheres [2]. This is caused by the structural change of the carbonaceous material during the carbonization process. By contrasts, the PC prepared using silica of 10 nm size shows a larger pore-size distribution than the

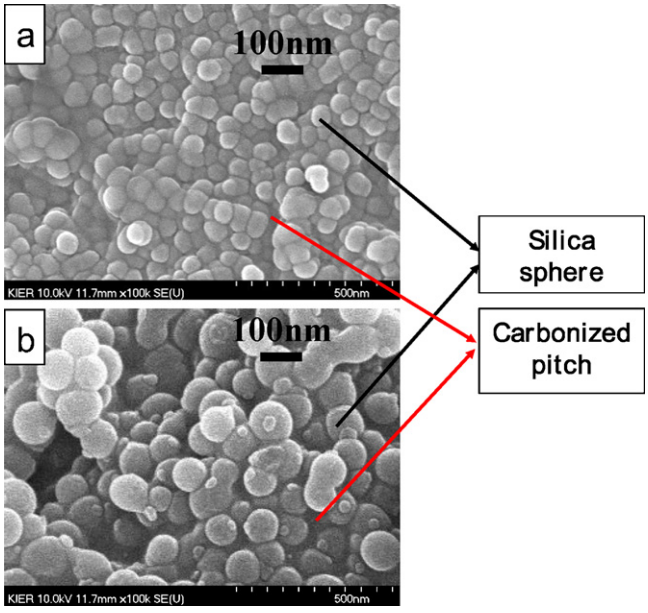

Fig. 4. Electron micrographs of carbonized pitch with silica after heat treatment at 1000 °C: (a) 40–50 nm; (b) 90–100 nm.

Table 1
Specific surface area and average pore diameter of PCs

Sample	Vulcan XC 72R	Raw pitch	K10	K20	K50	K100
S (BET, $m^2\ g^{-1}$)	254	1.8	273.2	212.4	132.9	88.2
S (micro)		0.2	26.4	29.6	9.6	6.6
S (meso–macro)		1.6	246.8	182.8	123.3	81.6
V (total)	0.39	0.00444	1.1545	0.9402	1.2302	0.2519
Average pore diameter ($4V/A$), nm	5.73	–	16.9	17. 7	37.0	80.8

original silica. This is due to some broken pores in the surface of the carbon and the greater development of open pores in the PC during the carbonization and etching processes.

3.2. Characteristic of Pt–Ru/PCs

X-ray diffraction patterns of the PCs prepared from raw pitch and the Pt–Ru/PCs are given in Fig. 7. As shown in Fig. 7(a), carbonized carbon using raw pitch has a typical soft-carbon structure with a high intensity at approximately $2\theta = 26^\circ$ [10]. The PCs, however, has a slightly amorphous structure compared with raw pitch. This is due to the mesopores and open pores in the carbon.

Guo et al. [11] obtained XRD patterns of Pt/C that exhibited diffraction peaks of (1 1 1), (2 0 0) and (2 2 0) at 2θ values of 39.9°, 46.3° and 67.45°, respectively. The diffraction patterns of the Pt–Ru catalyst supported on PCs (Fig. 7(b)) are similar to those of Pt/C, except that the 2θ values are shifted to slightly higher values [10,11]. Additionally, the structure of the Pt–Ru

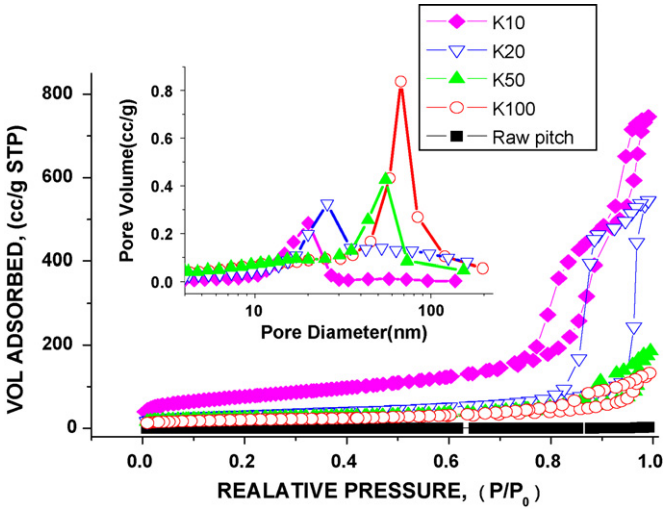

Fig. 6. Nitrogen adsorption isotherms of raw pitch and size-controlled PCs.

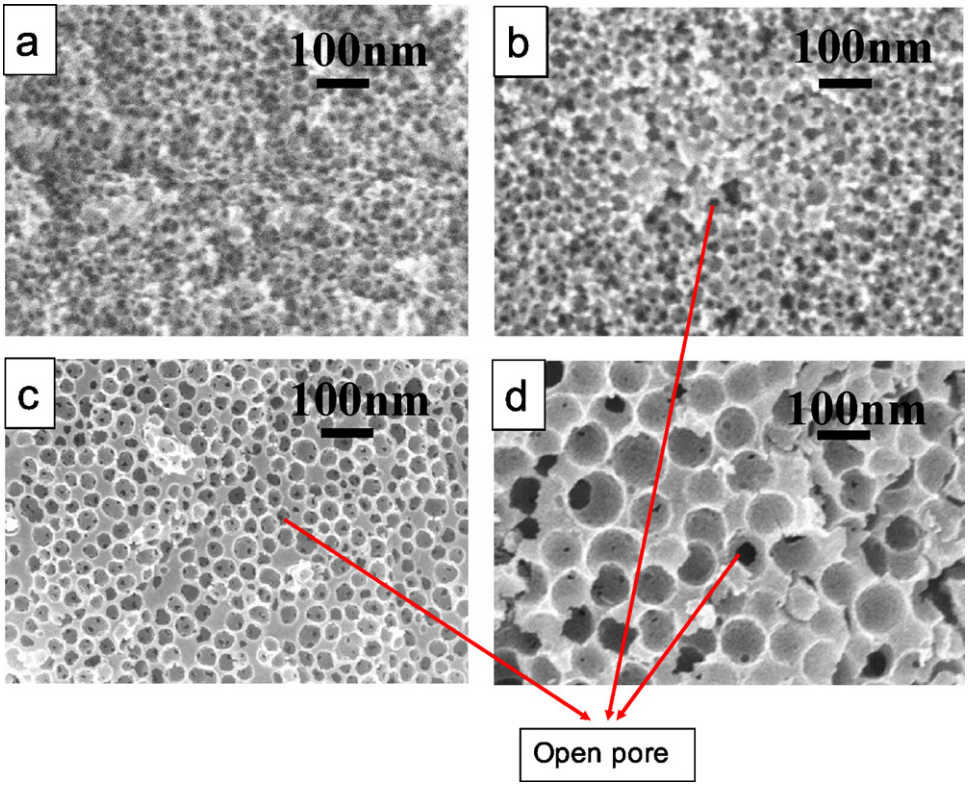

Fig. 5. Electron micrographs of carbonized PCs after etching of silica with NaOH: (a) 10–20 nm (K10); (b) 15–30 nm (K20); (c) 30–50 nm (K50); (d) 80–100 nm (K100).

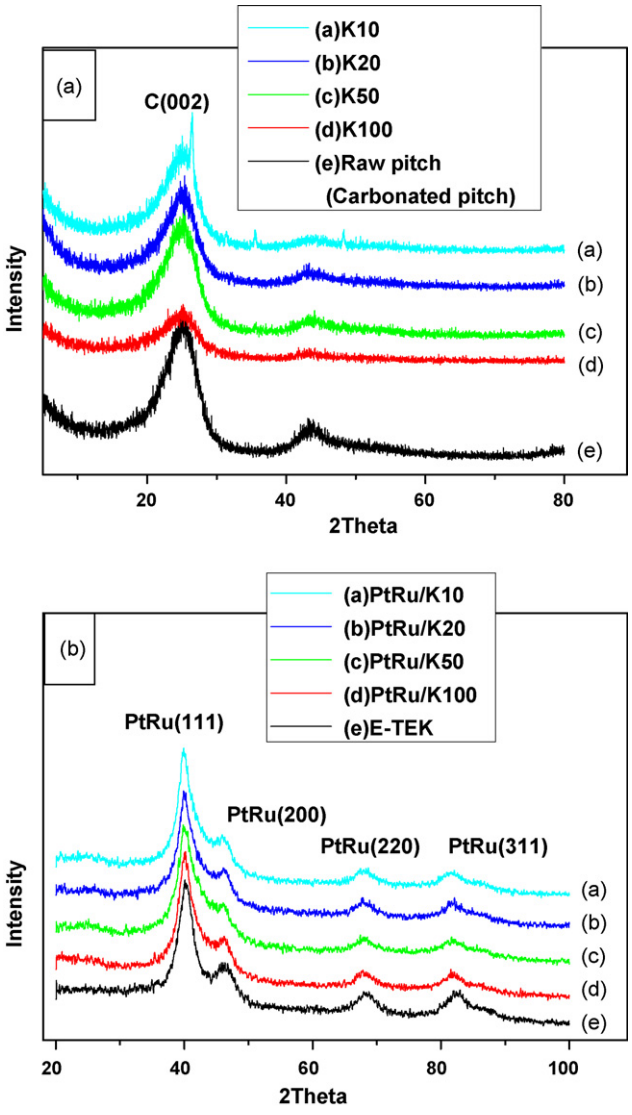

Fig. 7. X-ray diffraction patterns of (a) carbonized PCs with raw pitch and (b) Pt–Ru catalysts supported on PCs.

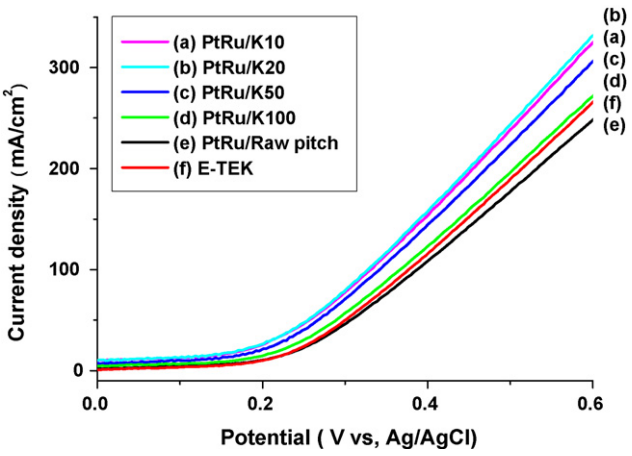

Fig. 8. Cyclic voltammograms of Pt–Ru catalysts supported on PCs.

catalyst is nearly identical to that of the commercial E-TEK catalyst.

The average particle size of Pt–Ru was determined using the (2 2 0) peak according to Scherrer's equation [12,13]. The particle sizes of the alloy and the specific surface areas of the Pt–Ru supported on PCs with different pore sizes, as calculated by XRD and the chemisorption method, are summarized in Table 2. The particle sizes of the Pt–Ru alloy increase from 2.6 to 3.0 nm when the pore size changes from 10 nm (K10) to 100 nm (K100).

The specific surface areas of the catalysts were calculated from the XRD data with the assumption that the Pt–Ru particles are spheres, as suggested by Roth [14]. The values increase from 88.9 to 102.6 nm on decreasing the particle size of the Pt–Ru alloy. This indicates that a Pt–Ru alloy with a smaller particle size can be obtained by using PC that is smaller than 20 nm in size.

The metal dispersion, crystallite size and metallic surface area of the Pt–Ru/PCs catalysts as tested using a chemisorption method are also summarized in Table 2. The metallic dispersion and surface area are increased when the pore size of the PCs is less than 20 nm. The crystallite size is decreased by decreasing the pore size of the carbon.

In summary, the Pt–Ru alloy supported on PC with a pore size of approximately 20 nm has the smallest particle size and the largest metallic surface area compare with the others.

3.3. Electrochemical characteristics of Pt–Ru/PCs

Cyclic voltammograms of the Pt–Ru catalysts supported on PCs with raw pitch are shown in Fig. 8 together with that of the commercial E-TEK catalyst supported on carbon black [14,15]. The K20 catalyst shows greater methanol oxidation activity at 0.4 V than K10, K50, K100 and the commercial E-TEK catalyst (60 wt.% Pt–Ru/Vulcan XC 72R). The methanol oxidation rates of Pt–Ru/K10, Pt–Ru/K20, Pt–Ru/K50 and the Pt–Ru/K100 cat-

Table 2
Properties of Pt–Ru/PCs obtained by XRD and chemisorption techniques

Techniques	E-TEK (Pt–Ru/Vulcan XC 72R)	Pt–Ru/K10	Pt–Ru/K20	Pt–Ru/K50	Pt–Ru/K100
XRD					
Pt–Ru alloy particle (nm)	2.7	2.6	2.6	2.8	3.0
Theoretical specific surface area ($m^2\ g^{-1}$ metal)	98.8	102.6	102.6	95.2	88.9
Chemisorption					
Metal dispersion (%)	8.8	7.8	7.9	6.1	5.5
Crystallite size (nm)	14.0	15.8	15.6	20.2	22.3
Metallic surface area ($m^2\ g^{-1}$ metal)	25.1	22.3	22.6	17.5	15.8

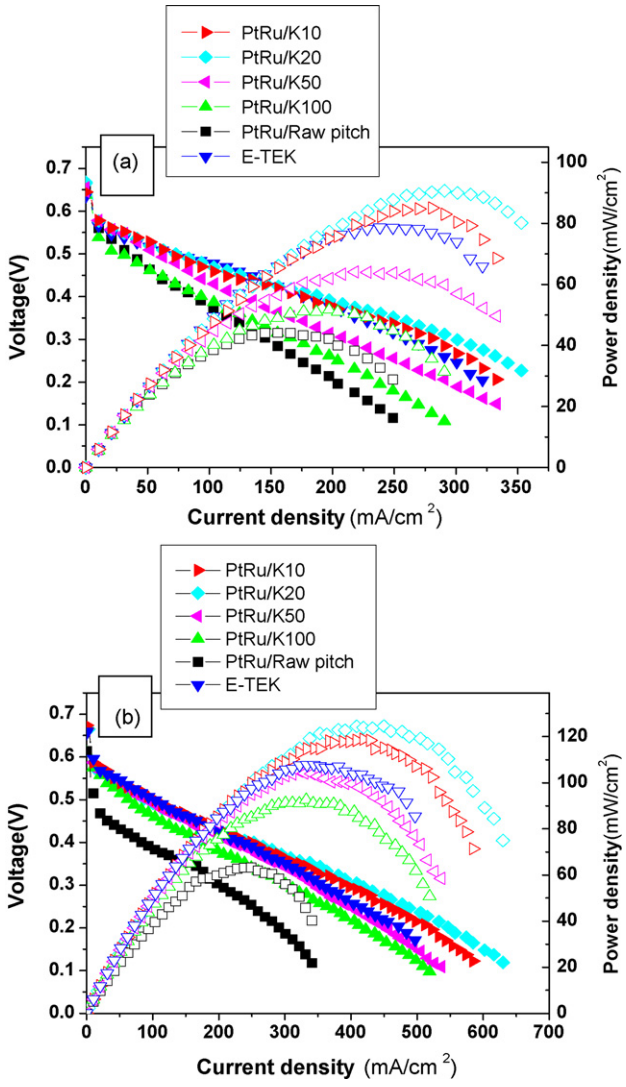

Fig. 9. Single-cell performance of DMFC in (a) air, (b) oxygen, 60 °C, open pressure. Anode: 2.0 M CH_3OH, 1.5 cm^3 min^{-1}; cathode: 330 cm^3 min^{-1} air, 250 cm^3 min^{-1} O_2.

alysts are about 45, 48, 40 and 30% higher than that of the Pt–Ru/raw pitch catalyst at a constant voltage of 0.4 V. All of the Pt–Ru/PCs showed greater levels of methanol electro-oxidation activity compared with the commercial E-TEK; in particular, the methanol oxidation rate of Pt–Ru/K20 is nearly 35% higher.

The current–voltage characteristics of single cells with different MEAs using Pt–Ru/PCs as the anode catalyst with air and oxygen as the oxidants at 60 °C are presented in Fig. 9. The results show a similar trend to those obtained from cyclic voltammetry. As the mesopore size of the PCs becomes smaller,

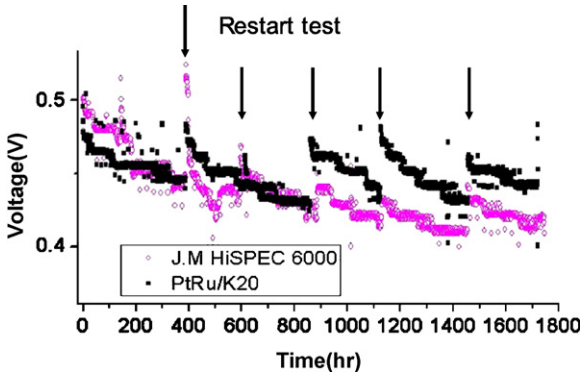

Fig. 10. Long-term durability test of single-cell performance of DMFC in air at 60 °C, open pressure. 80 mA cm^{-2}, anode: 1.0 M CH_3OH, 1.5 cm^3 min^{-1}; cathode: 300 cm^3 min^{-1}, air.

the performance of the single cell increases. The highest power density is obtained from K20, namely, 90 and 126 mW cm^{-2} using air and oxygen, respectively, at 60 °C. By comparison, the maximum power density of the commercial E-TEK catalyst is 79 and 108 mW cm^{-2} in air and oxygen, respectively, at 60 °C. The single-cell performance of Pt–Ru/K20 is 15–16% higher than that for the commercial E-TEK catalyst.

The greater performance of Pt–Ru/K20 can be attributed to many factors. An important factor is the effect of open pores in the PC that interconnects other pores. A Nafion solution filled in an open pore will transfer protons more easily from the anode side to the membrane than a closed pore such as carbon black or raw pitch. The smallest particle size and the largest metallic surface area compared with the other catalysts, as listed in Table 2, is an additional factor.

3.4. Analysis of durability tests

The durability of single cells prepared with Pt–Ru/K20 and the carbon black supported J.M (HiSPEC 6000) catalyst is shown in Fig. 10. The voltage of the single cell using the Pt–Ru/K20 catalyst is 0.48 V during the early stage of the test at a constant current density of 80 mA cm^{-2}. This value decreases as the operating time increases. When the operating time reaches 1700 h, the voltage is reduced to nearly 0.43 V, i.e., an approximate 10% loss. By comparison, the single-cell voltage of the J.M catalyst falls from 0.50 to 0.42 V (15% loss) at a constant current of 80 mA cm^{-2} for 1700 h. In addition, the single-cell voltage using the Pt–Ru/K20 catalyst is a higher than that of the J.M catalyst when the operating time surpasses 850 h. This indicates that the rate of activity loss of the J.M catalyst is higher than that of the Pt–Ru/K20 catalyst [20,23,24].

Table 3
XRD patterns of Pt–Ru/K20 and a commercial catalyst with a durability test

Catalysts	Pt–Ru alloy particle size (nm)		Theoretical specific surface area (m^2 g^{-1} metal)	
	Before test	After 1700 h	Before test	After 1700 h
Pt–Ru/K20	2.6	3.6	102.6	74.1
J.M HiSPEC 6000	1.9	3.0	140.4	88.9

The results of XRD analysis [12,14,23] after a lapse of 1700 h are shown in Table 3. The particle size of Pt–Ru supported on K20 increases from 2.6 to 3.6 nm, i.e., at a rate of about 38%. The particle size of Pt–Ru supported on carbon black (J.M catalyst) increases from 1.9 to 3.0 nm, i.e., at a rate of about 58%. The theoretical specific surface area of the Pt–Ru particles supported on K20 changes from 102.6 to 74.1 $m^2\ g^{-1}$ metal while that supported on carbon black decreases from 140.4 to 88.9 $m^2\ g^{-1}$ metal, i.e., decreasing rates of approximately 28 and 37%, respectively. From the above results, when Pt–Ru metals are supported on PC with a pore size of 20 nm, the aggregation rate of the metal particles is slower than that of metals supported on the carbon black. This is due to the different structures of the two carbon substrates [19].

4. Conclusions

Pore-size controlled PCs for catalyst supports in DMFCs are prepared from mesophase pitch using silica spheres of different sizes. The specific surface area of the PCs is 88.2–273.2 $m^2\ g^{-1}$ and the average pore diameter, which depends on the size of the silica spheres, varies from 15 to 100 nm.

A Pt–Ru alloy catalyst supported on PC with a pore size of approximately 20 nm shows the smallest particle size and the largest metallic surface area compare with the others.

The rate of methanol oxidation on Pt–Ru/K10, Pt–Ru/K20, Pt–Ru/K50 and the Pt–Ru/K100 catalysts is approximately 45, 48, 40 and 30% higher than that on Pt–Ru/non-porous pitch-based carbon at a constant voltage of 0.4 V. All Pt–Ru/PCs display higher rates of methanol electro-oxidation compared with commercial E-TEK and non-porous pitch-based carbon Pt–Ru catalysts.

The performance of single cells increases as the mesopore size of carbon decreases. The highest power density is obtained from K20 at 90 and 126 mW cm^{-2} using air and oxygen at 60 °C, respectively.

When a single cell is operated for nearly 1700 h, the particle size of Pt–Ru supported on K20 changes from 2.6 to 3.6 nm, while that of Pt–Ru supported on carbon black (J.M catalyst) increases from 1.9 to 3.0 nm. Thus, the rate of activity loss of the J.M catalyst is higher than that of Pt–Ru/K20. The latter shows excellent electrochemical stability during 1700 h compared with the commercial J.M catalyst.

Acknowledgement

This work was supported by the Core Technology Development Program for Fuel Cells of the Ministry of Commerce, Industry and Energy (MOCIE) in Korea.

References

[1] Z. Li, M. Jaroniec, Carbon 39 (2001) 2080–2082.
[2] T. Kyotani, Carbon 38 (2000) 269–286.
[3] S.A. Johnson, P.J. Ollivier, T.E. Mallouk, Science 283 (1999) 963–965.
[4] C.G. Chai, S.B. Yoon, J.S. Yu, J. Phys. Chem. B 108 (2004) 7074–7079.
[5] J.S. Yu, S.B. Yoon, G.S. Chai, Carbon 39 (2001) 1442–1446.
[6] M.S. Kim, S.B. Yoon, K.N. Sohn, J.Y. Kim, C.H. Shin, T.H. Hyeon, J.S. Yu, Micropor. Mesopor. Mater. 63 (2003) 1–9.
[7] J.Y. Kim, J.W. Lee, T.H. Hyeon, Carbon 42 (2004) 2711–2719.
[8] S.J. Han, M.S. Kim, T.H. Hyeon, Carbon 41 (2003) 1525–1532.
[9] S.J. Gregg, K.S.W. Sing, Adsorption, Surface Area and Porosity, 2nd ed., Academic Press, Inc., New York, 1982, pp. 111–194.
[10] E. Antolini, F. Cardellini, J. Alloys Compd. 315 (2001) 118–122.
[11] J.W. Guo, T.S. Zhao, J. Prabhuram, R. Chen, C.W. Wong, Electrochim. Acta 51 (2005) 754–763.
[12] B.D. Cullity, Elements of X-ray Diffraction, 2nd ed., Addison-Wesley Publishing Company, Inc., Canada, 1978, pp. 99–106.
[13] V. Radmilovic, H.A. Gasteiger, P.N. Ross, J. Catal. 154 (1995) 98–106.
[14] C. Roth, N. Martz, F. Hahn, J.M. Leger, C. Lamy, H. Fuess, J. Electrochem. Soc. 149 (2002) 433–439.
[15] Allen J. Bard, Larry R. Faulkner, Electrochemical Methods, 2nd ed., John Wiley & Sons, Inc., USA, 2001, pp. 226–234, 242–247.
[16] W.K. Peck, S.M. Park, Electrochemistry (Science and Technology of Electrode Processes), Revised ed., Cheong Moon Gak Publishers, Korea, 2001, pp. 137–151.
[17] D.H. Jung, C.H. Lee, C.S. Kim, D.R. Shin, J. Power Sources 71 (1998) 169–173.
[18] K.D. Nam, T.J. Kim, S.K. Kim, B.R. Lee, D.H. Peck, S.K. Ryu, D.H. Jung, J. Korean Ind. Eng. Chem. 17 (2006) 223–228.
[19] D.H. Jung, J.H. Jung, S.H. Hong, D.H. Peck, D.R. Shin, E.S. Kim, Carbon Sci. 4 (2003) 121–125.
[20] D.H. Jung, S.Y. Cho, D.H. Peck, D.R. Shin, J.S. Kim, J. Power Sources 106 (2002) 173–177.
[21] S.D. Knights, K.M. Colbow, J.S. Pierre, D.P. Wilkinson, J. Power Sources 127 (2004) 127–134.
[22] T. Poppe, Icarus 164 (2003) 139–148.
[23] W. Chen, G. Sun, J. Guo, X. Zhao, S. Yan, J. Tian, S. Tang, Z. Zhou, Q. Xin, Electrochim. Acta 51 (2006) 2391–2399.
[24] H. Kim, S.J. Shin, Y.G. Park, J.H. Song, H.T. Kim, J. Power Sources 160 (2006) 440–445.